GENTLE WAVY DEFECTS IN KNURLED WOUND ROLLS

By

Kevin Cole
Optimation Technology, Inc.
USA

ABSTRACT

The manufacture of many products involves the winding of continuous thin, flexible webs into wound rolls. In many applications involving the use of plastic webs, it is beneficial to mechanically emboss the edges of the web prior to winding so as to provide a thickening of the web in these areas. During and after winding, radial pressures developed in the wound roll then are concentrated in the localized embossed areas. This reduces the sensitivity to the formation of web distortions due to stress concentrations that would otherwise develop due to lengthwise persistent widthwise thickness nonuniformities. One of the drawbacks of this process is that the wound roll is now more sensitive to buckling-type defects owing to reduced interlayer pressures in the bulk of the roll away from the embossed edges. In this paper, we present results for a particular type of web defect known as a *Gentle Wavy Defect* (*GWD*) that forms in the wound roll due to presence of axial corrugations that develop in the wound roll. We begin by presenting product and process information characterizing this situation along with potential theories as to the cause of the corrugations and GWDs. Next, we provide results from numerous experiments that provide guidance on the likely mechanism responsible for the formation of the roll and web defects. Through these experiments and the application of winding models, we then demonstrate the cause of the defects and provide guidelines on how to avoid them in future applications.

NOMENCLATURE

a	single layer thickness
A	area
C	moisture concentration
C_e	equilibrium moisture concentration corresponding to local vapor pressure
C_i	time-dependant moisture concentration at node-n
C_o	moisture concentration at time t = 0

D	diffusion coefficient
F	rate of transfer of moisture per unit area of section
Q_{ib}	moisture flow into layer from adjacent layer toward the node-1 side
Q_{it}	moisture flow into layer from adjacent layer toward the node-n side
S	surface moisture transfer coefficient
t	time
x	space coordinate

INTRODUCTION

Wound rolls are used to package and transport webs from one process to another and ultimately, to the end-use customer. In order to reliably and cost-effectively maintain web quality through these processes, it is incumbent that the winding processes be optimized in terms of process and product settings. Historically, this is done through a combination of empirical testing and experience. In addition, first-principle wound-roll models have been developed to assist with this optimization by providing insight into the relationships between the factors influencing roll and web quality in terms of clearly identifiable wound roll and web imperfections.

Owing to the importance of winding, in terms of the pervasive extent of this process, and the complexity of winding, both in terms of the many ways rolls can be wound and in terms of the many types of defects that can result, there is a wealth of literature published dealing with the subject. However, this information can be difficult to access owing to the diverse terminology. Following Good and Roisum [1], winding equipment can be described in terms of arrangements and classes. Arrangements deal with functional applications such as manufacturing and converting while classes deal with the methods used to apply forces necessary to wind the web. Typical arrangements would include turret winders (high speed manufacturing), reels (continuous manufacturing, typically at the end of paper base machines), duplex winders (commonly used as offline rewinders), salvage winders (used to evaluate or save rolls by rewinding), etc. Winding classes would include pure centerwinding, layon roller assisted centerwinding, surface winding, and combination center-surface winding [1]. An excellent reference for roll and web defects is D. Smith et al [2]. In this reference, it is seen that many winding and web defects are an interconnected function of product factors, winding equipment arrangements and classes. For example, baggy lanes are caused by excessive web deformation due to ridges in wound rolls that are in turn formed from lengthwise persistent gage profile variation. Baggy lanes tend to be worse on winding arrangements that utilize a layon roller.

The subject of this paper is the study of a particular problem noted during a web manufacturing process shown schematically in Figure 1. Cellulose Triacetate (CTA) web is first manufactured in a continuous casting process and is wound using a two spindle turret winder operating in the centerwinding mode. Subsequently, rolls are unwound into a converting line where an aqueous gelatin coating is continuously applied to the web, dried and wound using a two spindle turret winder equipped with an undriven nip roller. Prior to winding, the web passes beneath a scanner which utilizes infrared radiation to assess the flatness of the continuously coated web. Webs manufactured in this fashion possess flatness which meets customer requirements.

However, not all rolls manufactured on the converting line follow this simple two step process. Approximately 15% of the rolls off the casting line are first rewound on a salvage winder using one spindle operating in the centerwinding mode. Rolls are rewound to insure quality of the final product and are typically identified by concerns noted during the initial manufacturing process. Approximately 25% of these rewound rolls experience the defect that is the subject of this paper. The defect, referred to as a *Gentle Wavy Defect*

(GWD), is characterized by the scanner as a transverse direction (TD) buckle that is approximately 1 to 2 cm in width in the machine direction (MD) and approximately a quarter to three quarters of the width of the web in length in the TD direction. The defect occurs in clusters at various distances along the length of the web. Through a preliminary assessment, it was quickly determined that the GWD defect originates in axial corrugations present in rolls wound on the salvage winder but not in the casting process winder. Figure 2 shows a typical example of a GWD defect.

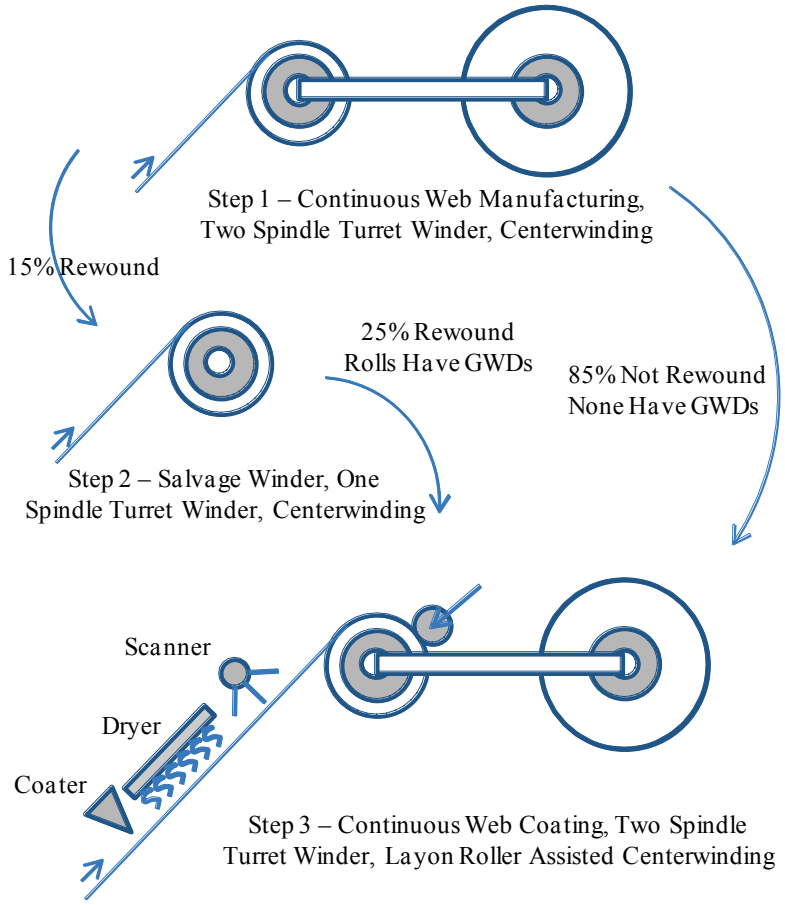

Figure 1 – Cellulose Triacetate Web Manufacturing Process Flow Schematic

While the GWD defect has similarities to two defects noted in [2], it is not the same for various reasons. The first defect, *TD wrinkles,* are web buckles that extend to the edges of the web and arise due to *TD corrugations* that likewise extend to the edges of the roll. GWDs never extend to the edges but instead are restricted to the inside portion of the web. The second defect, *Center Buckles*, have the same general appearance as GWDs, however, they are more gradual in MD profile and are more randomly distributed; furthermore, they arise from the method of manufacture of the sheet and not from axial corrugations in the wound roll.

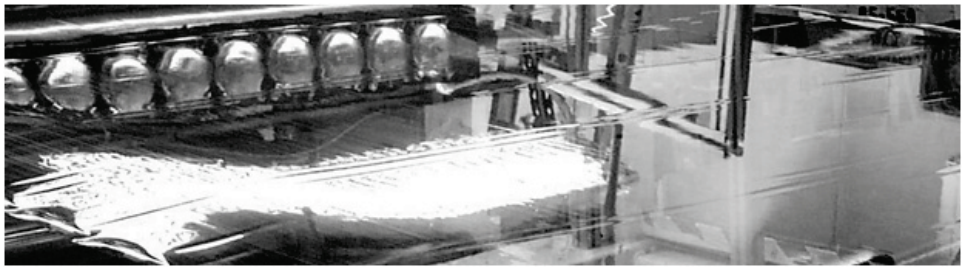

Figure 2 – Typical Gentle Wavy Defect (GWD)

Details of the casting and salvage winding processes and some of the physical characteristics of the CTA web are presented in Table 1. It is of special importance that the web casting line utilizes edge knurling (Figure 3) to provide interlayer pressure relief across the middle of the web during winding in the casting line. This is a well known process, Hawkins [3], that is employed in web manufacturing to prevent lengthwise persistent gage profile variation from developing into ridges leading to baggy lanes prior to the coating process. Figures 4 and 5 show the winding speed and tension for the casting and salvage winding processes respectively. It is of interest to note that while the winding speed is constant for the casting winding process, the speed is variable for the salvage winding process. In fact, the situation is often more complex than shown in Figure 5 owing to the need to visually observe selected areas of the web for the presence of defects unrelated to GWDs. The potential implications of variable speeds during salvage winding will be discussed in more detail in the next section.

This paper describes experimental and analytical methods employed to understand the causes of GWDs and to develop options to modify the manufacturing process to eliminate them. First, theories are presented as potential explanations for the formation of GWDs. Next, process data is described that provided guidance as to which theory was the most likely explanation for the GWDs. More detailed experimental results are then presented that further refined our understanding of the causal mechanism. Analysis using predictive winding models is then described and applied to investigate process improvement options. Results and conclusions are finally presented.

GWD FORMATION THEORIES

GWDs are permanent deformations in the web that arise from axial corrugations in the wound roll that either are created during or after winding on the salvage winder. Knowing this, it then remains to determine the source of the axial corrugations. From the knowledge of the product and the process, several ideas are potential candidates. Before discussing these, some additional background information is presented. At the time of this problem, data from the converting line suggested that the GWDs were dependent on which casting line the rolls were manufactured on. This information led to the identification of several product related variables such as front-to-back web friction, web camber, web thickness widthwise thickness nonuniformity, and knurl height.

Three potential hypotheses were put forth as the likely candidates for the formation of axial corrugations and GWDs. First, it was theorized that perhaps a shift had occurred in one of the product related variables and that had led to an increased likelihood of the formation of axial corrugations on the salvage winder. It is known from experience that knurled roll winding is a very sensitive process and that specifications on many of the product variables must be maintained to avoid any of a number of potential defects.

However, careful review of production data did not reveal any noticeable changes in the product variables and furthermore, there were no discernable differences between the webs manufactured on the two casting machines. Thus, it had to be concluded that there was some other cause for the axial corrugations and also that the observation that there were differences between the performance of rolls from the two casting lines needed further investigation.

Web Type	Cellulose Triacetate		
Web Thickness, μm	133.4	Casting Winding Process:	
Web Width, m	1.384	Winding Speed, mpm	6.706 – Figure 4
Knurl Width, mm	9.525	Winding Profile	Constant tension, constant torque
Knurl Thickness, μm	Variable – Figure 3	Winding Tension	Variable – Figure 4
Effective Thickness, μm	139.6	Salvage Winding Process:	
Roll Length, m	1878	Winding Speed, mpm	Variable – Figure 5
Core OD, mm	156.3	Winding Profile	Constant tension, linear decreasing tension with radius
Roll OD, mm	598.6	Winding Tension	Variable – Figure 5

Table 1 – CTA Physical Dimensions and Winding Process Conditions

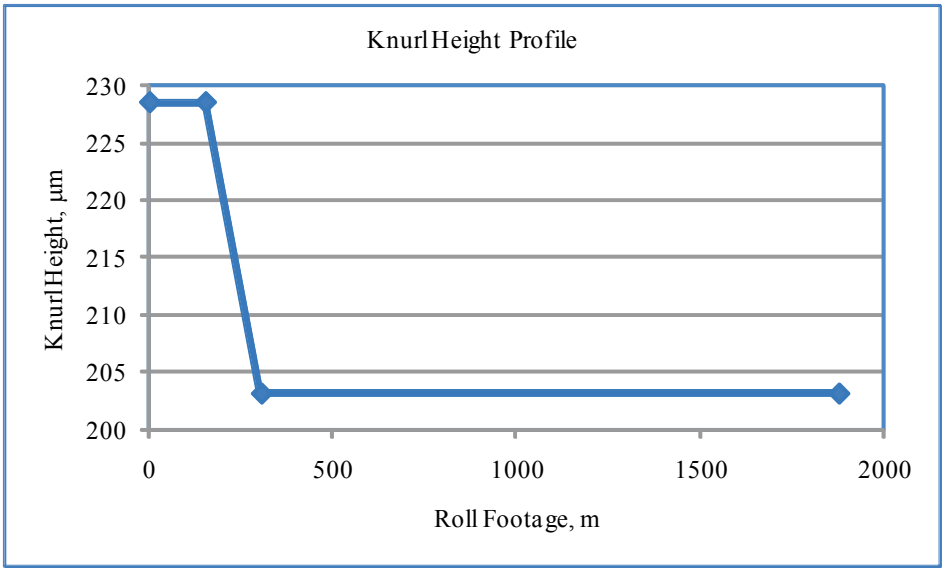

Figure 3 – Knurl Height Profile vs Roll Footage

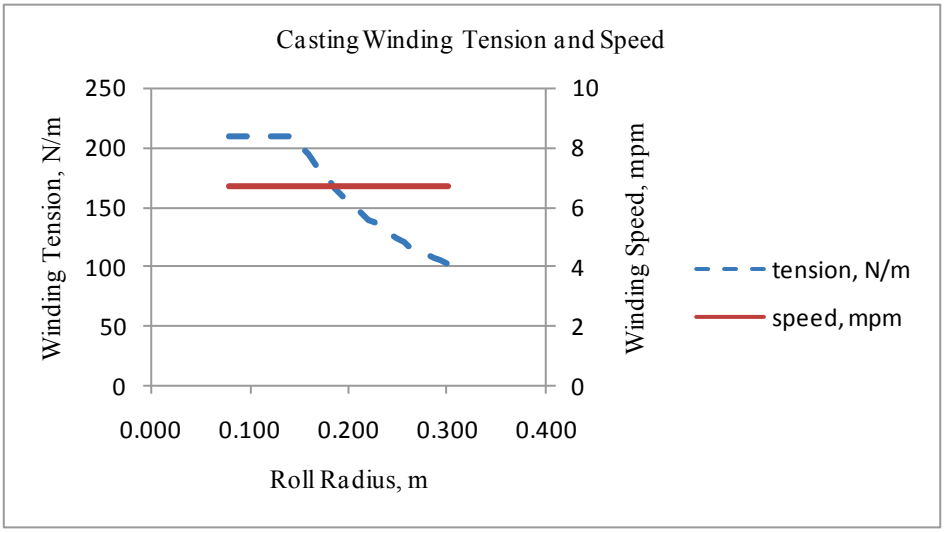

Figure 4 – Casting Winding Tension and Speed vs Roll Radius

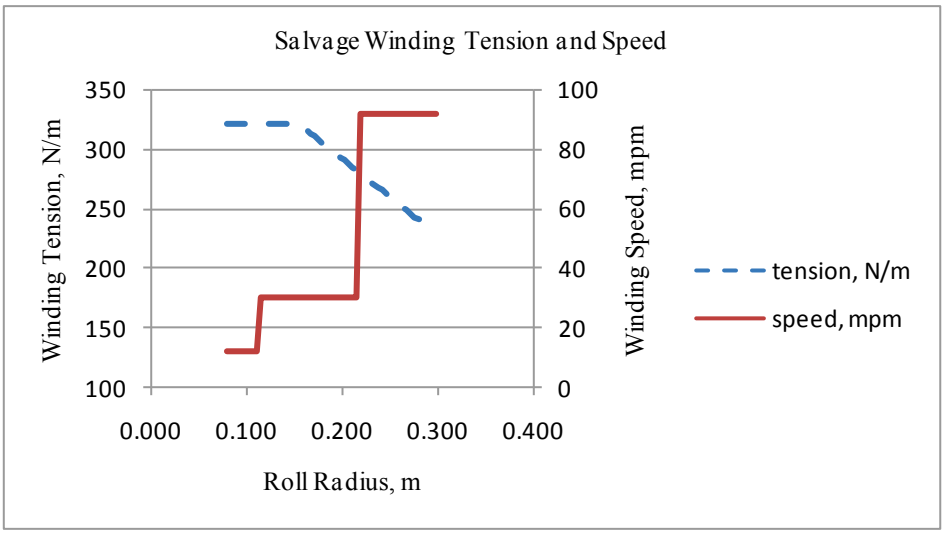

Figure 5 – Salvage Winding Tension and Speed vs Roll Radius

The second hypothesis arose from the observation that GWDs were only observed on rolls that were rewound on the salvage winder. From Figure 5, it has been noted that speed during normal operation is variable with increases occurring twice during winding. In addition, there are often times that the speed is changed in an even more extreme fashion. During these changes in speed, no attempt is made to adjust winding tensions. Thus, the relative contribution of air entrainment to the stresses developed in the winding roll changes. The impact of this change will lead to varying hardness within the winding roll and consequently, it was theorized that this was the source of the axial buckles. The effect of air entrainment on roll stresses is described by Lei et al [6] where an air entrainment wound roll model is presented. From that work, it was shown that the total pressure between layers within a wound roll can be separated into two components: contact pressure and air pressure. As winding speed increases, the contact pressure decreases. To maintain a consistent contact pressure variation within the wound roll, winding tensions would therefore have to be adjusted appropriately to compensate for speed changes. In the next section, an empirical test is described that suggested that this hypothesis was not sufficient to explain the formation of axial corrugations.

The third hypothesis arose from further observations of GWD data. Figure 6 presents results from 25 rolls wound on the salvage winder. The vertical axis represents whether or not GWDs were present in a particular roll and the horizontal axis represents whether or not the salvage winder came to a complete stop during rewinding of the roll.

Figure 6 – GWD vs Salvage Winder Speed

The data indicates that for GWDs to occur, the salvage winder must come to a complete stop. However, while a necessary condition, stoppage of the salvage winder does not always lead to GWDs. Two things can be inferred from this. First, if the second hypothesis were true, then one would expect that GWDs would be present on some of the rewound rolls that didn't stop but got sufficiently low in speed. This would be expected since the effect described in the second hypothesis is a continuous function of speed and not an on-off effect as the results in Figure 6 seem to imply. Thus, the fact that no rolls had GWDs where the salvage winder was moving strongly implies that variations in salvage winder speed that are uncompensated by tension changes is not the cause of GWDs. This conclusion was verified by results in the next section. The second inference is obvious: another hypothesis, one that depends on the stoppage of the salvage winder, was needed to explain the presence of the axial corrugations and the formation of GWDs. Thus, a third hypothesis, more general than the first two, was put forth stating that the cause of axial corrugations was due to stoppage of the salvage winder during the rewind operation. Figure 6 shows this to be true. However, the question is what is it about stopping the salvage winder that leads to axial corrugations. Some potential causes that were suggested include: dramatic tension changes at zero speed (e.g., slack web), acceleration/deceleration effects (e.g., brake application prior to the roll coming to a stop), and web tracking effects (e.g., sudden shifts in lateral position due to tension changes or improper guider control as zero speed). In the next section, experiments are described which were conducted with the intent of isolating the cause of the problem. As will be shown, these results led to a conclusion that was not considered at the outset of the work.

EXPERIMENTAL PROCESS STUDIES

In order to develop insight into the cause(s) of the axial corrugations and GWDs, it was decided that more controlled experiments were needed. For this purpose, a standardized rewinding process was developed and a sequence of experiments performed. The standardized procedure is presented in Figure 7. The procedure consists of a sequence of stops, starts, reverses, and speed changes during the rewinding process. After

completion of winding, the roll is stored for 1 week and then subsequently rewound a second time and evaluated for GWDs. The evaluation is done visually by evaluating GWD severity in the free span just upstream of the salvage winder. Note that footage is measured from the salvage winding start. By doing a controlled rewinding operation, much more quantitative information was able to be collected and significant insight into the cause of axial corrugations and GWDs was developed.

1. Set machine at standard winding tension conditions and run the machine at normal speed conditions for the first 152 m (500 feet).
2. At 152 m (500 feet) stop with tension on, wait 1 minute, then ramp to 61.0 mpm (200 fpm).
3. At 244 m (800 feet) stop, back up 91.4 m (300 feet) stop, then go forward 91.4 m (300 feet), stop for 1 minute, then ramp up to 45.7 mpm (150 fpm).
4. At 366 m (1200 feet) stop, wait 3 minutes, then ramp up to 61.0 mpm (200 fpm).
5. At 610 m (2000 feet) stop, wait 1 minute, back up 91.4 m (300 feet), stop, wait 1 minute, then go forward 91.4 m (300 feet), stop, wait 2 minutes, ramp up to 61.0 mpm (200 fpm).
6. At 762 m (2500 feet) stop, wait 5 minutes, ramp up to 91.4 mpm (300 fpm).
7. At 1070 m (3500 feet), repeat step 5.
8. At 1370 m (4500 feet), repeat step 6.
9. At 1680 m (5500 feet), repeat step 5.
10. Store roll for one week, rewind on the Salvage Winder and make GWD observations

Figure 7a – Salvage Winder Standard Test Process Conditions, written

Figure 8 shows the results from the first roll rewound on the salvage winder using the standardized procedure. Shown on the graph is GWD severity (0 – no GWD, 1 – light GWD, 2 – medium GWD, 3 – severe GWD) and total stoppage time as a function of roll footage measured from the salvage winder start. Several items of immediate interest are observed. First, GWDs are only seen in locations where stops are made to the salvage winder. Furthermore, the severity of the GWDs (and extent) appears to be correlated to the magnitude of stoppage time. For example, on both occasions when the stoppage time was 5 minutes, the GWDs were the most severe. Figure 9 confirms this correlation where the extent of the GWDs (radial height and footage) are plotted as a function of stoppage time. The correlation between GWD severity and stoppage time is strong. The remaining observation is that the GWDs formed in the roll nearer to the core than the stoppage point. During evaluation of the roll, the unwinding roll was also observed. In all cases where GWDs were observed, axial corrugations were seen in the unwinding roll. This confirmed the correlation between axial corrugations and GWDs.

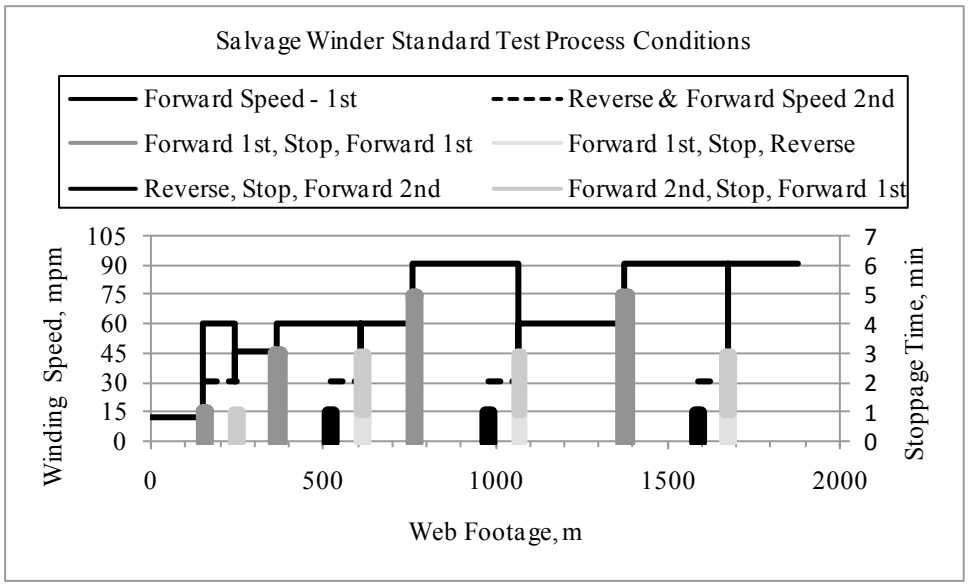

Figure 7b – Salvage Winder Standard Test Process Conditions, graphical

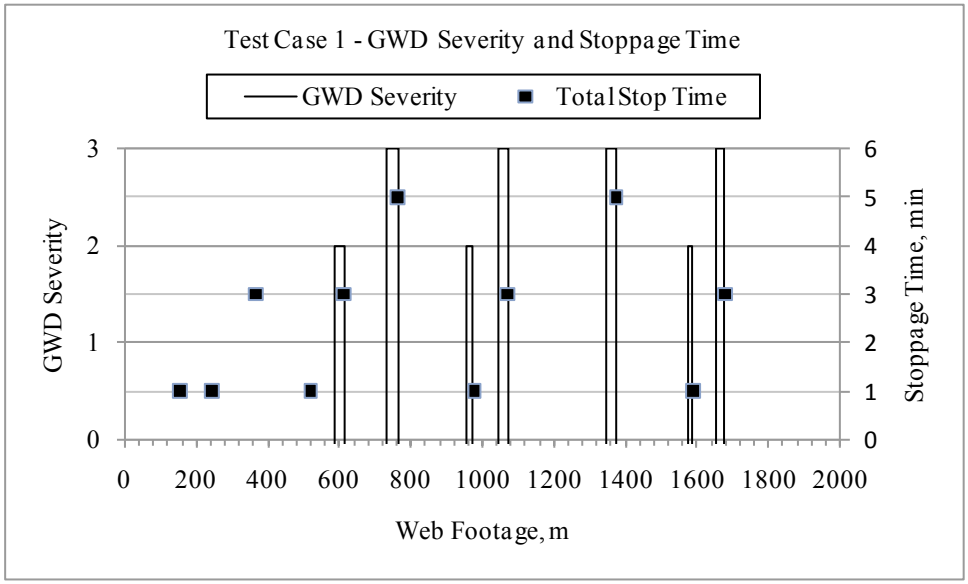

Figure 8 – Test Case 1 GWD Severity and Stoppage Time vs Web Footage

Based on these observations, several additional test cases were conducted in an effort to isolate the cause of the axial corrugations and GWDs. A listing of these cases are shown in Table 2. The purpose of each of these trials was to determine the relative importance of various potential causes of the axial corrugations and GWDs. Each trial is summarized in Table 2 by the following: (a) a description of the trial – what process variable was being evaluated, (b) a measure of the GWD severity – the cumulative sum of

the product of the defect severity and the footage at each location where GWDs were seen, (c) the number of events (or occurrences) where GWDs were seen in the roll, (d) the roll length, and (e) a statement of the relative performance with respect to the base case. Cases 2 and 5 were run in an attempt to confirm the supposition that the problem was not explainable in terms of hypothesis 2 in the previous section. These cases represent two attempts at adjusting tension as a function of speed. In the first, case 2, the controls were modified so that tension was proportional to speed such that at zero speed, the tension was 30% of the setpoint value shown in Figure 4. Results indicated that this actually made the GWDs worse. This was contrary to expectation and did not solve the problem. In the second case, the controls were again modified so that the winding tension was maintained at setpoint until the salvage winder stopped. Subsequently, the tension was dropped to 30% of setpoint and then subsequently ramped back to setpoint over a footage of 61 m. This footage compares to the normal ramp footage of 23 m at an acceleration rate of 3 mpm/sec up to a speed of 91 mpm. Some improvement is noted relative to the first attempt at modifying the tension profile; however, the results are very comparable to the baseline case. Taken together, these two results suggest that perhaps a solution could be found by modifying tension in the other direction; e.g., raising it when ramping in speeds lower than setpoint. However, no further attempts were made as it was still suspected that something else was responsible for the axial corrugations and GWDs since the defects were still only seen when the speed of the rewinder went to zero and was held there for some length of time. This is demonstrated clearly in Figure 10 where GWD severity and total stoppage time as a function of roll footage measured from the salvage winder start are shown for case 2.

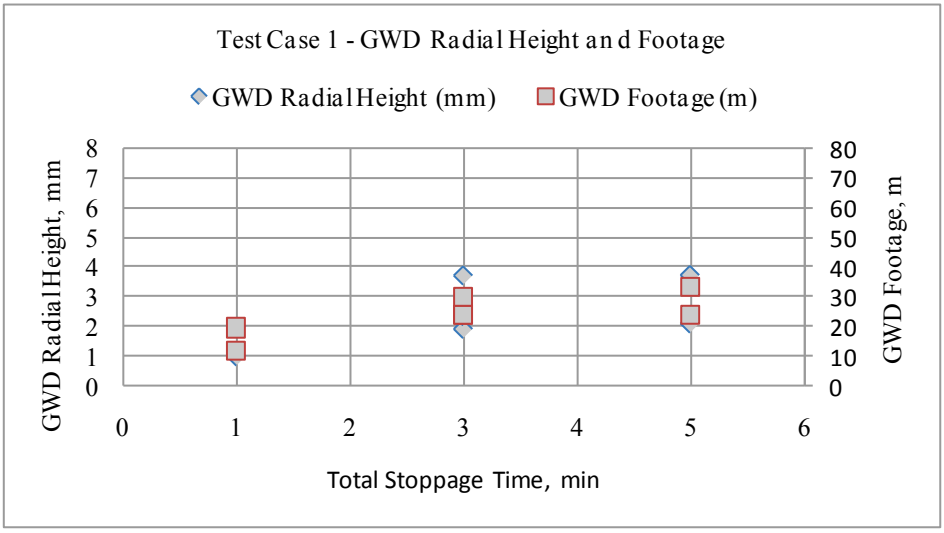

Figure 9 – Test Case 1 GWD Radial Height and Footage vs Total Stoppage

Cases 3 and 4 were trials made to determine if the GWDs problem was unique to the casting line and salvage winder. In case 3, a roll was rewound on a different salvage winder. The objective was to determine if there were unique problems with the primary salvage winder or if the problem was rewinder independent. Results indicated somewhat better performance but not the elimination of the problem. Again, the GWDs were only seen in areas closer to the rewinder core corresponding to locations where the rewinder

was stopped. In case 4, a roll from a different casting line was rewound on the primary salvage rewinder. In this case, the performance was worse than the baseline case. The results of these two cases again confirmed that a stoppage of the rewinder for some amount of time was required to generate axial corrugations and GWDs.

Case	Comment	Severity x Footage (severity × m)	Events	Roll Length (m)	Observations
1	baseline	445	7	1878	baseline
2	tension proportional to speed	703	9	1780	worst case
3	different salvage winder	323	7	1870	better than baseline
4	different casting line	637	7	1664	worse than baseline
5	tension ramped over 61 m after stop	462	9	1878	comparable to baseline
6	verification 1	476	9	1878	comparable to baseline
7	verification 2	70	2	1878	significant improvement

Table 2 – Salvage Winder Experimental Cases

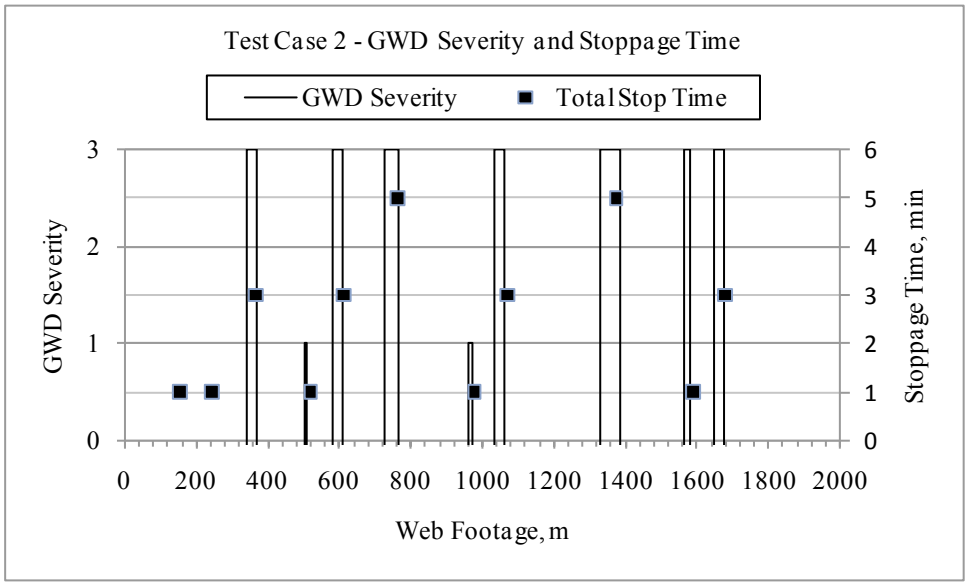

Figure 10 – Test Case 2 GWD Severity and Stoppage Time vs Web Footage

Before discussing cases 6 and 7, labeled as verification experiments, it is important to note that at this point a curious observation made during the evaluation of the baseline case suddenly became quite illuminating. Figure 11 shows a picture of the sidewall of the case 1 rewound roll at the rewinder prior to the one week post rewind evaluation. The salvage rewinder utilizes a single edge guider system and this edge is the nonguided side during winding. Careful examination of the unguided edge indicates an offset at each radial location where the roll was stopped during the initial rewind process. At the time, it was thought perhaps this was a guider problem but upon further evaluation, it was

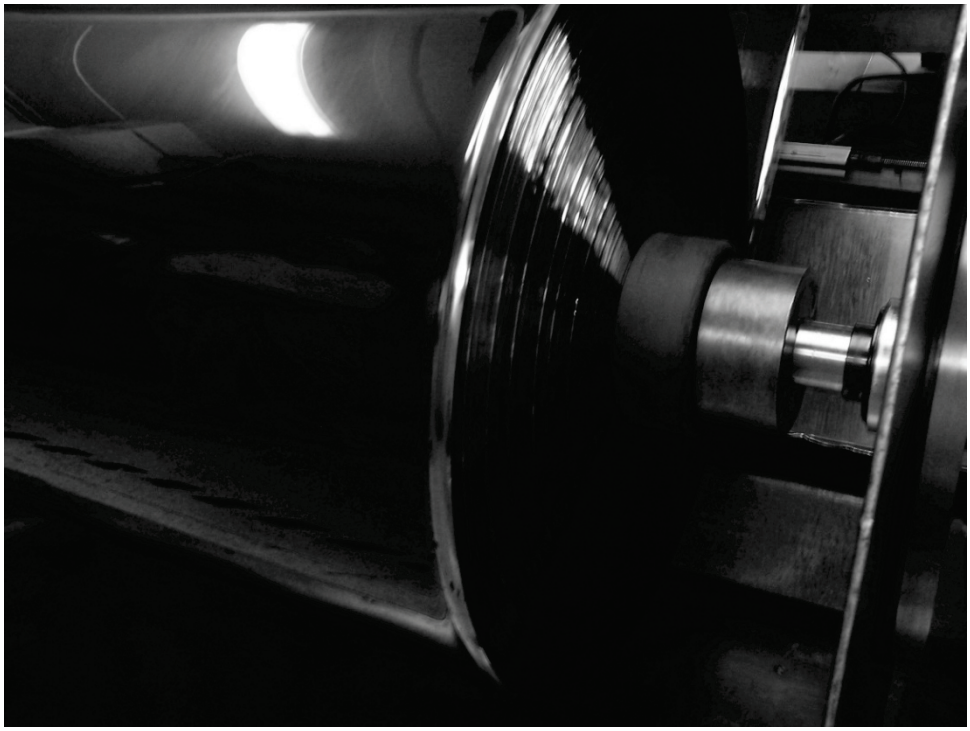

Figure 11 – Test Case 1 Rewound Roll, Unguided Edge Prior to Evaluation

determined that in fact the web actually was wider at each of these locations. Subsequent reflection on the cause and implication of this phenomena led to a refinement of the third hypothesis. To explain the refinement, it is helpful to describe one further aspect of the casting line and rewinder process. During the initial casting process, Cellulose Triacetate web enters the winder section at extremely low moisture content (~0.3% by weight, 5% RH at 72°F). Prior to winding, the web is exposed for approximately 1 minute (7 m) to ambient conditions which vary between seasonal extremes from a minimum of 20% RH (uncontrolled, winter) to a maximum of 55% RH (controlled down by a chilled water system, summer). During this exposure, the web absorbs a very small amount of additional moisture and essentially remains at 5% RH when wound. During the rewinding process, the ambient moisture conditions range between 35% RH (controlled up by steam system, winter) and 45% (controlled down by a chilled water system, summer). Thus, the web absorbs varying amounts of moisture depending on the stoppage time and since CTA is very hygroscopic, the web grows isotropically in the length and width direction. Subsequently, the web is wound onto the existing partially rewound roll. After winding,

the web that has absorbed moisture, 12.8 m in length, now loses moisture by diffusion into the bulk of the roll that is at the much lower moisture level that it was initially wound at. Reduction of moisture then leads to a reduction in length and width. Consequently, the layers that are experiencing a reduction in width and length act to radially compress the roll closer to the core. This is much like heat shrinking a ring onto the existing roll. The result is the hypothesis that the layers underneath are driven into compression leading to axial corrugations and the formation of GWDs. In the next section, analytical results are presented that confirm the validity of this hypothesis.

With this understanding, two further cases were undertaken to empirically confirm this hypothesis. Both cases were attempts at running the rewinder experiment at significantly reduced levels of RH. In case 6, the rewinder was at 23% RH and in case 7, the rewinder was at 13%. This compares to the baseline case where the rewinder was at 33% RH. The lower RH levels were achieved by conducting the experiments on days when the external temperature and dew point were low (e.g., in the winter) and then piping in external air through a heat exchanger into the rewinder without humidification. From the results of Table 2, it is seen that in fact the second verification experiment resulted in a very significant reduction in GWDs. This is shown in Figure 12. During the verification experiments, the change in width was measured. Table 3 shows calculations of the hygroscopic coefficient of expansion using the empirical data. As the data indicates, the results are in very good agreement with laboratory measurement of the hygroscopic coefficient of expansion.

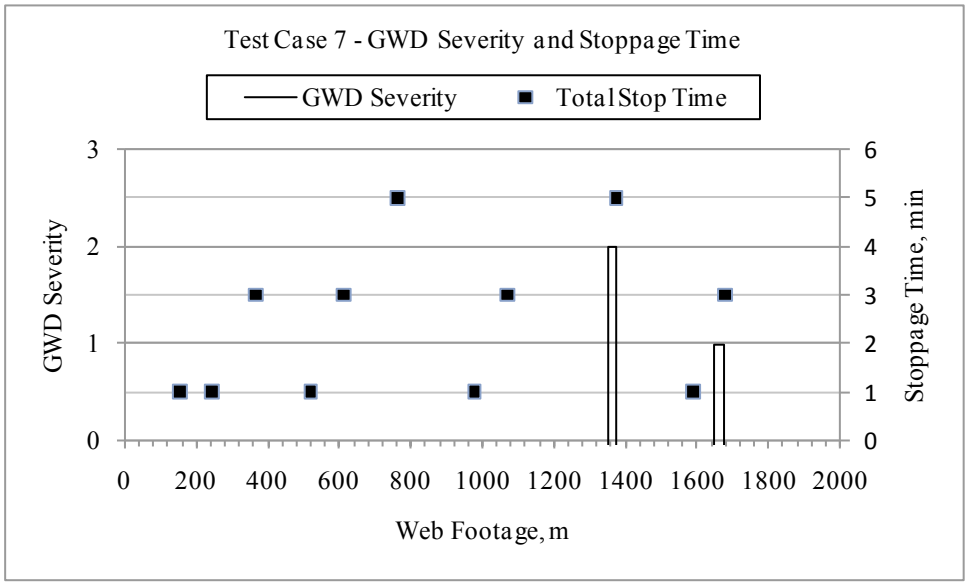

Figure 12 – Test Case 7 GWD Severity and Stoppage Time vs Web Footage

ANALYTICAL MODELING

Moisture Diffusion Governing Equations

Moisture diffusion is the process by which matter, in this case water, is transported from one part of a system to another as the result of a variation in concentration of the diffusing substance. The mathematical theory of diffusion in isotropic substances is based on the hypothesis that the rate of transfer of the diffusing substance through a unit area of

a section is proportional to the concentration gradient measured normal to the section, Crank [4]:

$$F = -D\frac{\partial c}{\partial x} \qquad \{1\}$$

where F is the rate of transfer per unit area of section, C is the concentration of moisture, x the space coordinate measured normal to the section, and D is the diffusion coefficient. If F, the amount of moisture diffusing, and C, the concentration, are expressed in terms of the same unit of quantity, e.g. gram or moisture concentration $\left(\frac{moisture\ by\ weight}{dry\ TAC\ by\ weight}\right)$, then it is clear from equation {1} that D is independent of this unit and has dimensions *(length)^2(time)$^{-1}$*, e.g. *m^2/sec*. The negative sign in equation {1} arises because diffusion occurs in the direction opposite to that of increasing concentration.

Case	Comment	Casting %RH	Rewind %RH	Diff %RH	Equil Diff %RH	Width Change, mm	α, m/m/%RH
1	baseline	5	38	33	9.67	0.91	0.000068
6	verification 1	5	28	23	6.74	0.46	0.000049
7	verification 2	5	18	13	3.81	0.23	0.000043
	Time (min)	5	Moisture Equilibrium, %		29.3	Width, m	1.38
		lab hygroscopic expansion coefficient:					0.000055

Table 3 – Empirical Calculation of the Hygroscopic Coefficient of Expansion

The differential equation of diffusion is derived from equation {1} by considering a control volume where the amount of moisture flow into and out of the control volume is balanced by the rate of change of moisture in the control volume. If the diffusion gradient is one-dimensional, then there is:

$$\frac{\partial C}{\partial t} + \frac{\partial F}{\partial x} = 0 \qquad \{2\}$$

Substitution of equation {1} into equation {2} yields the differential equation for diffusion:

$$\frac{\partial C}{\partial t} = \frac{\partial}{\partial x}\left(D\frac{\partial C}{\partial x}\right) \qquad \{3\}$$

Initial and boundary conditions are required to solve equation {3}. Following Liu and Simpson [5], these conditions are given as follows. The initial condition is:

$$C = C_o \quad (0 \le x \le a, t = 0) \qquad \{4\}$$

where C_o is the constant concentration in the web in the free span upstream of the salvage winder or in the layers in the wound roll comprised of the web previously in the free span during a stoppage of the salvage winder (Figure 13). The boundary conditions are:

$$D\frac{\partial C}{\partial x} = S(C_e - C) \quad (x = 0, a; t > 0) \qquad \{5\}$$

where a is the thickness of the web in the free span upstream of the salvage winder or in the layers in the wound roll comprised of the web previously in the free span during a stoppage of the salvage winder. S is the surface moisture transfer coefficient and C_e is the equilibrium concentration in the CTA web corresponding to the vapor pressure in the environment remote from the surface of the sheet.

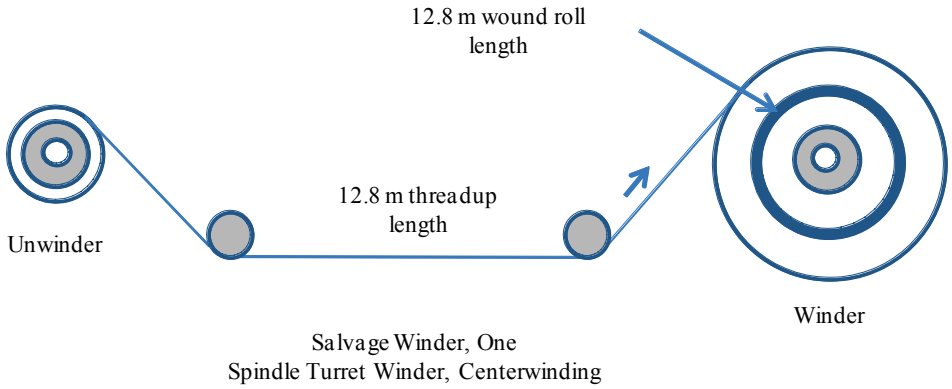

Figure 13 – Moisture Diffusion Geometry

Moisture Diffusion Solution

From Figure 13, the solution to equations {3} through {5} depend on whether moisture is being absorbed by the web in the salvage winder free span (equations {3} through {5} apply) or given up by the web to the wound roll (equations {3} and {4} apply). In the second case, the initial condition for $x < 0$ and $x > a$ is the concentration established at the casting line windup.

To solve the diffusion equations, the procedure is as follows. First, the thickness undergoing diffusion is divided into arbitrary layers. The center of each layer is called a "node" and is numbered from 1 to n. Each layer has thickness x_i. From equation {3}, the rate of change of moisture in each layer is governed by:

$$Ax_i\frac{dC_i}{dt} = Q_{ib} + Q_{it} \qquad \{6\}$$

where:

A is the area of each layer, m^2
x_i is the thickness of each layer, m
C_i is the moisture concentration at center, *unitless*
Q_{ib} is the moisture flow into the layer from the adjacent layer toward the node-1 side, or from ambient air if node 1

Q_{it} is the moisture flow into the layer from the adjacent layer toward the node-n side, or from ambient air if node n

and:

$$Q_{ib} = \frac{DA}{\frac{x_i}{2} + \frac{x_{i-1}}{2}}\left(C_{i-1} - C_i\right) \quad if\ i > 1$$

$$Q_{ib} = SA\left(C_e - C_1\right) \quad if\ i = 1 \qquad \{7\}$$

$$Q_{it} = \frac{DA}{\frac{x_i}{2} + \frac{x_{i+1}}{2}}\left(C_{i+1} - C_i\right) \quad if\ i < n$$

$$Q_{it} = SA\left(C_e - C_n\right) \quad if\ i = n$$

Equations {6} and {7} form a system of n linear first-order constant-coefficient differential equations in the n scalar variables $C_1, C_2, \ldots, C_n$ that are solved using the commercially available program Matlab™. Solution is straightforward but to achieve solution accuracy, care must be taken in the selection of layer thickness. Typically, accurate results can be achieved by using very thin layers near boundaries, thicker layers away from boundaries where diffusion proceeds more slowly and by not varying thicknesses between adjacent layers by more than a factor of 2.

Empirical Determination of D and S

For the CTA, empirical moisture conditioning data was used to estimate the diffusion coefficient and the surface moisture transfer coefficient. Figure 14 presents empirical data and corresponding analytical data using the model of the previous section. The empirical data is the normalized amount of moisture pickup as a function of time. The data is for a single layer with equilibration occurring at both surfaces. The sheet was initially equilibrated at a moisture concentration corresponding to 5% RH and then subsequently exposed to a moisture concentration corresponding to 50% RH. The tests were performed at 21 deg C. An optimizer was used to determine D and S such that the error between the model predictions and the empirical data was minimized. From this analysis, the value of D was computed to be 3.7677e-10 *m^2/sec* and the value of S was computed to be 7.3175e-8 *m/sec*. It is of interest to note that the moisture diffusion behavior of CTA, while driven by the moisture concentration, can correspondingly be thought to be driven by relative humidity since the relationship between moisture concentration and relative humidity is essentially linear. Further, moisture content in TAC web at any given relative humidity depends very little on temperature (unlike air). Figure 15 shows moisture concentration as a function of RH for three different temperatures. As a result of the linear correspondence between moisture concentration and RH, the time dependent moisture concentration distributions from the diffusion model of the next section are translated to RH and then used as inputs to the winding modeling simulation of subsequent section.

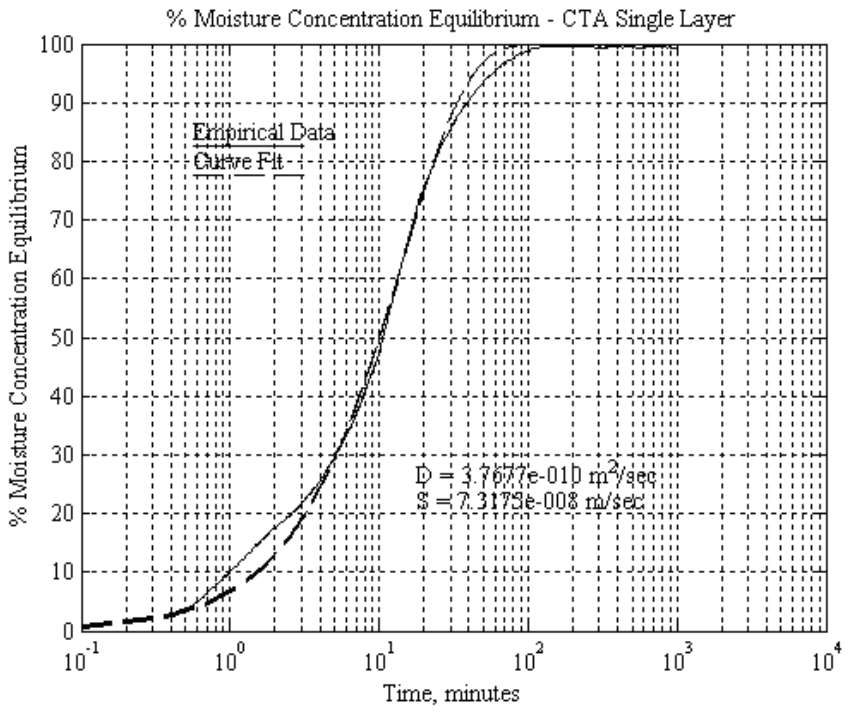

Figure 14 – Empirical Determination of *D* and *S*

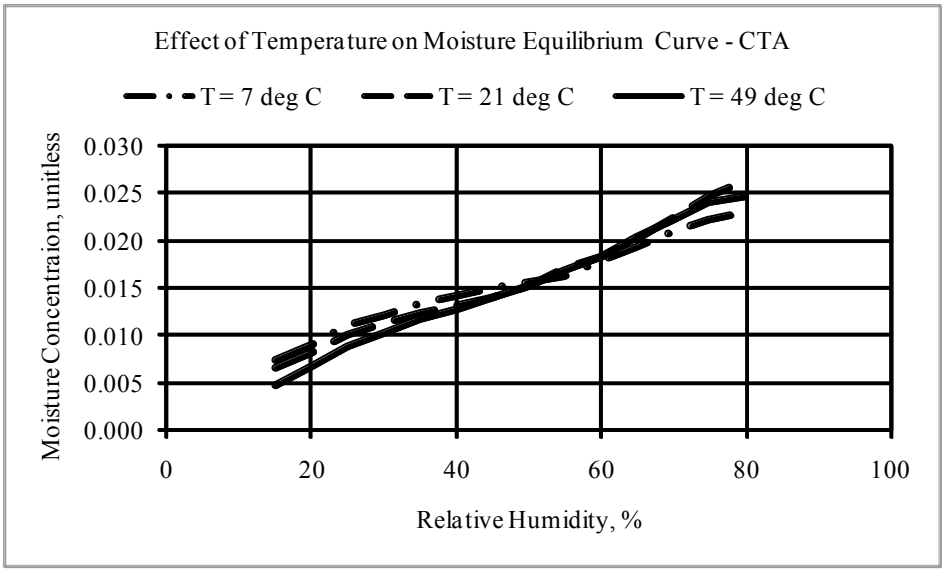

Figure 15 – Effect of Temperature on Moisture Equilibrium Curve – CTA

Analysis of Moisture Distribution – Figure 7 Standard Winding Process

In Table 4, the moisture concentration developed in the salvage winder threadup during the Standard Winding Process shown in Figure 7 for the baseline and verification cases is presented. The results are for a stoppage time of five minutes and provide initial conditions for the determination of transient moisture distributions using the moisture diffusion model after the web is subsequently wound into the roll on the salvage winder. Figure 16 shows the distribution of RH for two of the three cases: baseline and verification 2. The analysis was performed at a footage of 1372 m. The curves are for times ranging from 0 minutes to 10,000 minutes and are equally spaced in log time. These transients are used as inputs to the winding model simulations in the next section.

Case	Comment	Casting %RH	Rewind %RH	Equil Diff %RH	Layer %RH	Casting Moisture	Layer Moisture
1	baseline	5	38	9.67	14.67	1.79E-03	6.09E-
6	verification 1	5	28	6.74	11.74	1.79E-03	4.79E-
7	verification 2	5	18	3.81	8.81	1.79E-03	3.46E-
	Time (min)	5	Moisture Equilibrium, %		29.3		

Table 4 – Moisture Concentration in Threadup During Standard Test

Winding Modeling

The thermoelastic model with air entrainment developed by Lei and Cole [6] is used to simulate the in-roll tension stresses developed during initial rewinding on the salvage winder and subsequently due to moisture equilibration. The model is appropriate to study moisture effects since hygroelastic and thermoelastic effects are governed by the same mathematical theory. The objective is to illustrate that the mechanism of GWD formation presented previously is consistent with the stresses developed in the knurled wound roll. In Table 5, the material properties used in the winding model simulation are given. Table 6 gives the clearance and roughness moduli for both the knurled and unknurled sections of the web. In-roll tension stresses for the baseline case and the verification cases are presented in Figure 17. Observation of the results indicate that the in-roll tension stress is significantly negative for the baseline case away from the area in the roll previously exposed to the salvage rewinder environment during the stoppage of the salvage rewinder. The impact appears to be more significant towards the core. The stress is less negative for the first verification experiment. For the second verification experiment, the stress in the impacted area is no longer negative with no discernable difference compared to the baseline case. In all the cases, the in-roll tension stress in the affected area becomes positive owing to the length reduction driven by moisture loss to the surrounding roll. Based on the fact that negative in-roll tension stress is required to drive TD corrugations, the relative differences in performance between the GWD performance of the three cases modeled are in good agreement with the predicted in-roll tension stresses.

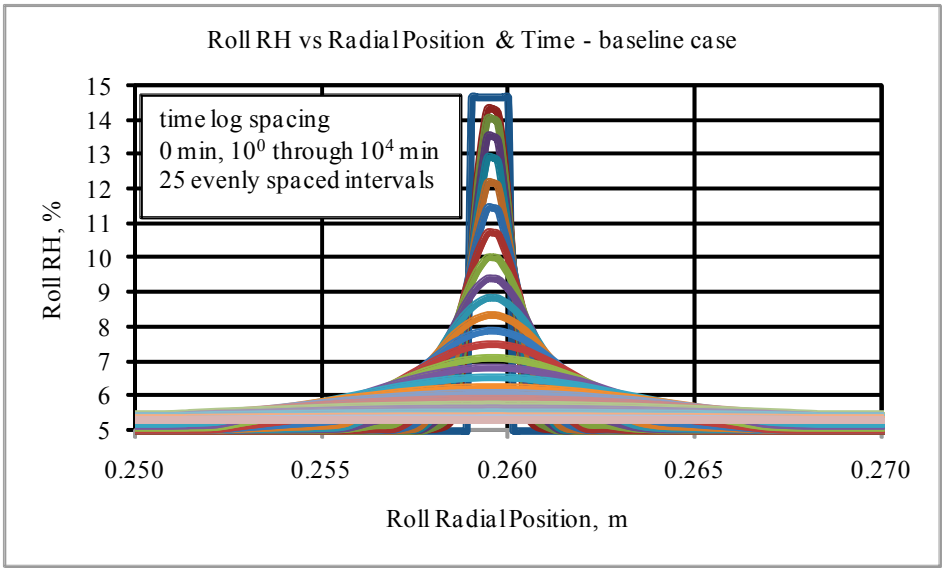

Figure 16a – Roll RH vs Radial Position & Time, 1371.6 m & 5 min Stop, Baseline

DISCUSSION

The ultimate objective of the work of this paper was to develop solutions to the GWD problem. Based on the findings, there are a combination of three changes that practically can be considered as viable options: (a) lower RH in the salvage rewinder (most effective), (b) reduce stoppage time in the salvage rewinder (second most effective owing to the continued need to evaluate web for quality), (c) reduce time in rewound roll format (least effective owing to rapid equilibration and therefore expected formation of axial corrugations). A fourth option of reducing time in the casting line windup isn't practical owing to the very short time in the windup and the large capital cost associated with either lengthening the conveyance path or increasing the RH of the casting line windup environment. Also, higher RH during winding in the casting line leads to a higher likelihood of other defects. Ultimately, the decision was made to modify the rewinding process to reduce stoppage time and further investigation is currently underway to develop the cost/benefit tradeoffs for further reducing the salvage rewinder RH.

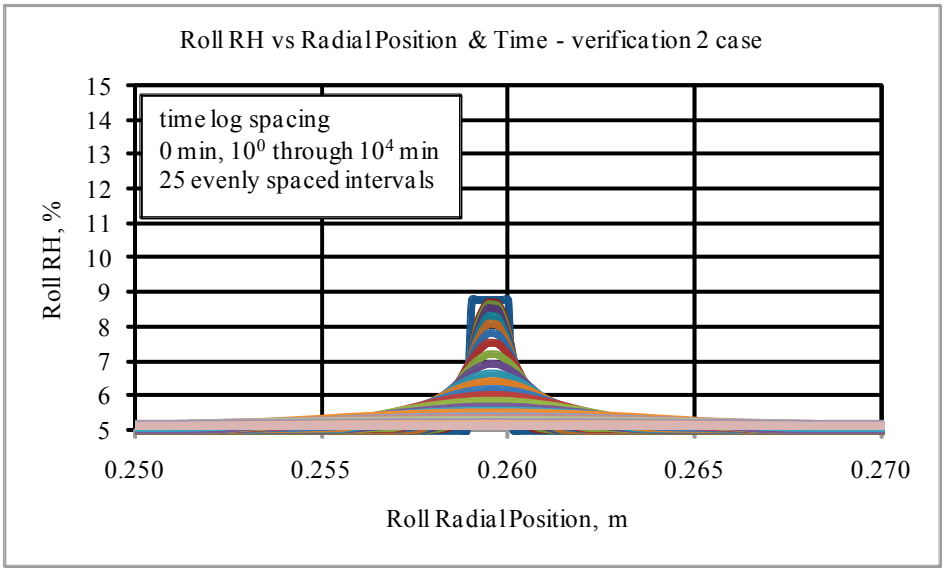

Figure 16b – Roll RH vs Radial Position & Time, 1371.6 m & 5 min Stop, Verification 2

CONCLUSIONS

The source of axial corrugations and GWDs in knurled roll winding during salvage rewinding has been identified and studied empirically and analytically. The primary cause of the defect is the highly hygroscopic nature of the CTA web. Stoppage during rewinding leads to moisture-induced growth of the web prior to rewinding. Subsequently, internal moisture diffusion results in shortening of the affected web leading to the development of significant and localized reduction of in-roll tension leading to axial buckling and GWDs. The presence of knurls, used to meet other process and product requirements, accentuates the GWD problem. Potential solutions consist of a combination of salvage rewind process modifications to reduce exposure time and equipment capital changes to reduce RH in the salvage rewinder.

Core Diameter (m)	0.156	Poisson Ratio of Stack	0.01
Roll Diameter (m)	0.599	Bulk Modulus (Gap)	2.83
Nominal Web Thick	140	Young's Modulus (GPa)	4.69
Number of Laps	1583	Core Modulus (GPa)	4.41
Knurled Web		Unknurled Web	
Air Film Ref Clear (μm)	36.3	Air Film Ref Clear (μm)	7.84
Contact Ref Clear (μm)	36.3	Contact Ref Clear (μm)	7.84
Total Web Thick (μm)	168	Total Web Thick (μm)	140
Circum Web Thick (μm)	132	Circum Web Thick (μm)	132
Section Width (mm)	12.70	Section Width (mm)	1356

Table 5 – Material Properties Used in Winding Modeling

REFERENCES

1. Good, J. K., Roisum, D. R., Winding: Machines, Mechanics and Measurements, DEStech Publications, Inc., 2007.
2. Smith, R. D., Roll and Web Defect Terminology, 2nd Edition, Tappi Press, 2006.
3. Hawkins, W., The Plastic Film and Foil Web Handling Guide, CRC Press, 2003.
4. Crank, J., The Mathematics of Diffusion, 2nd Edition, Oxford Science Publications, 1975.
5. Liu, J. Y., Simpson, W. T., "Solutions of Diffusion Equation with Constant Diffusion and Surface Emission Coefficients," Drying Technology, 15(10), 1997, pp. 2459-2477.
6. Lei, H., Cole, K. A., "A Thermoelastic Winding Model with Air Entrainment." Proceedings of the Sixth International Conference on Web Handling, Web Handling Research Center, Stillwater, Oklahoma, June 10-13, 2001.

Knurled Web			Unknurled Web		
Contact Clearance, μm	Contact Pressure, MPa	Stack Modulus, MPa	Contact Clearance, μm	Contact Pressure, MPa	Stack Modulus, MPa
36.271	0.000	0.059	7.838	0.000	0.029
27.051	0.028	0.373	2.063	0.028	0.211
22.139	0.138	1.467	0.971	0.138	2.185
15.093	0.689	4.562	0.339	0.689	19.898
1.648	5.516	50.945	0.026	5.516	654.928

Table 6 – Roughness Modulus of the Web Excluding Air Effect

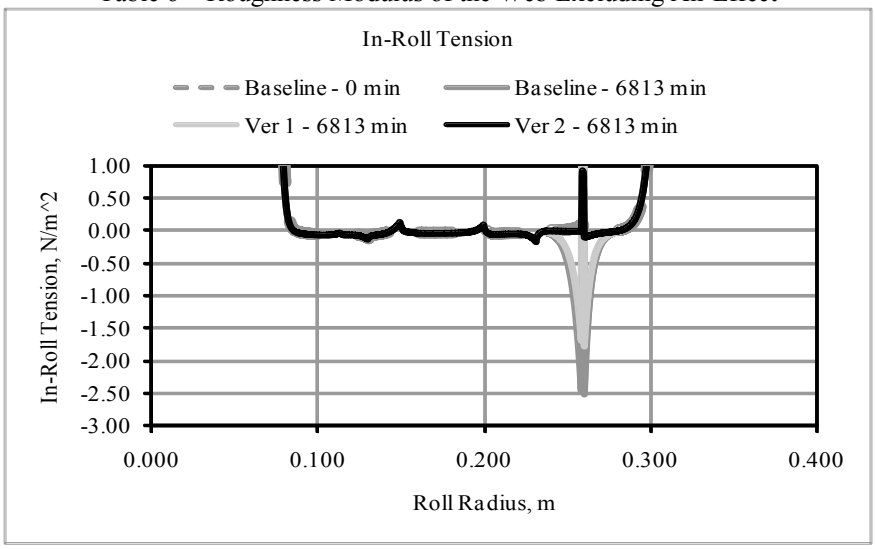

Figure 17 – In-Roll Tension vs Roll Radius, Cases 1, 6, 7

Gentle Wavy Defects in Knurled Wound Rolls	**K. Cole**, Optimation Technology, Inc., USA

Name & Affiliation	**Question**
Bob Lucas, Winder Science	In the paper industry it is not uncommon that moisture growth of a web can occur in the period required to make a web splice, especially if the mill is located geographically in a region where the humidity is high already. Web splices can require periods of two minutes to complete. In these cases enclosures are used around the winder to control the humidity and the web growth during the splice period. The question relative to your study regards when the web comes to a stop or slows down the viscoelastic behavior will be affected by the draw or tension set point and the residence time of the web in conditions where the humidity could be high. Have you considered this in the viscoelastic behavior?
Name & Affiliation	**Answer**
Kevin Cole, Optimation Technology	No, I have not considered it. Normally what is done on the salvage winder is that we drop tension. When stopping for more than a few seconds, they'll drop the tension to 30% of the run value. We do this to manage the behavior you describe. This particular web will take on moisture/humidity when sitting at the outside of the roll. This effect is well known. What I discussed today is not the only cause of gentle wavy defects in roll winding. We have had other episodes with these defects in the past where stops and starts were not required. More work is required for those cases.
Name & Affiliation	**Question**
Steve Lange, Procter & Gamble	Can you explain why you didn't see wrinkles in the cross-machine direction and only in the axial direction?
Name & Affiliation	**Answer**
Kevin Cole, Optimation Technology	My model did not include axial effects. Lateral shrinkage will take place. However, the knurled areas probably prevent sliding in the axial direction due to the high interlayer pressure in the knurl areas.